International Journal Of Engineering Research And Development
e- ISSN: 2278-067X, p-ISSN: 2278-800X, www.ijerd.com
Volume 17, Issue 3 (May-June 2021), PP. 35-42

An Image-based Locator for Detecting Regions of Disease-Related Patterns with Color Visualization of Shape in Medical Imaging

Peifang Guo
Montreal, QC, Canada

ABSTRACT.
In this paper, an image-based locator using the graphic color region growth procedure for segmentation (CRGPS) is proposed to detect positions of segmented disease-related patterns, including multiple intracranial electrodes implanted for the location of the seizure onset zone with epilepsy in stereo-electroencephalography (SEEG) and brain tumors in magnetic resonance imaging (MRI). In the proposed CRGPS method, the procedure of partitioning a color image into graphic regions of color is based on average values of colors in the graphic color region growth process. Then the image region projection operation is preformed to locate graphic regions of the segmented disease-related patterns in the X-Y coordinate plane on the basis of the image greyscale transformation. The experimental results not only succeed in localizing positions of the brain tumor regions in MRI and implanted intracranial electrodes used for tracing epilepsy in SEEG, but also exhibit the capability of enhancing the segmentation performance with color visualization of disease-related patterns. This study might provide unique insight with color vision to probe the depths of graphic regions of seizure focus with implanted intracranial electrodes in SEEG and brain tumors in MRI, which might have the potential to detect locations of disease-related patterns of interest graphically as markers for the early diagnoses of disease in medical imaging.

Date of Submission: 28-05-2021 Date of Acceptance: 10-06-2021

I. INTRODUCTION

Neurological disorders affect as many as one billion people worldwide, which could be diagnosed according to the primary location affected and the primary type of dysfunction involved. Among them, there are more than 600 diseases that connect the nervous system, including brain tumors and epilepsy. According to Health Canada, every day, 27 Canadians are diagnosed with brain tumors. There are over 120 different types of brain tumors, making medical diagnoses and effective treatment very complicated. In addition, the aggressive brain tumor is one of the leading causes of death in children under the age of 20 and the third leading cause of solid cancer death in young adults ages 20-39. The medical diagnoses for patients with brain tumors depend on a number of factors, including locations of tumor in the brain. The surgeons usually need to make a small hole in the skull and then guides a needle to the tumors in the brain, in order to find the exact locations of the brain tumors for a biopsy for medical interventions and treatments (Bauer, et al., 2013; Bakas, et al., 2017; Egger et al., 2013).

Among neurological disorders, epilepsy is a central nervous system disorder that causes seizures or periods of unusual behavior. The onset of epilepsy is common in children and older adults in general, but the condition can occur at any age. According to the World Health Organization, 50 million people have epilepsy. Since epilepsy is caused by some abnormal activities in the brain, seizures would affect any process the brain coordinates. Because seizure symptoms could vary widely for the brains of people with epilepsy, one of the challenges in achieving successful surgical outcomes in patients with epilepsy is the ability to appropriately localize the seizure onset zone (SOZ), including multiple intracranial electrodes implanted for epilepsy for localizing the SOZ in stereo-electroencephalography (SEEG), for the early diagnoses of the type of an epilepsy. (Wang, et al., 2021; Grecoa, et al., 2018; Ryvlin, et al., 2014; Bahi-Buisson, et al., 2008).

It might be useful to design an image-based locator for detecting positions of disease-related patterns with color visualization of shape graphically in the modalities of medical imaging, e.g., brain tumors in magnetic resonance imaging (MRI) and multiple intracranial electrodes implanted for epilepsy in SEEG, for the early diagnoses. In image processing, one application of the segmentation in color image is the localization of graphic image pattern positions and regions, in which the pixels belonging to a region of image pattern have the same color. For a color image, each category of pixels of colors denotes a region of the original pattern related to an image pattern to be classified in segmentation (for example, brain tumors in MRI and multiple electrodes implanted for epilepsy in SEEG in this study). Hence, the designs of segmentation algorithms in medical imaging would play an essential role in the acceleration of progress to benefit the discovery of disease-related

patterns with position for neurological diseases (Guo, at al., 2018; Gerard, et al., 2017; Ahmed, et al., 2015; Weiner, et al., 2013; West, et al., 2012).

There are various segmentation methods in the applications of neuroscience in medical imaging, including the manual work in a slice-by-slice manner (Egger, et al., 2013), the thresholding (Tohka, 2014; Rafael, et al., 2008), the morphology (Gui, et al., 2012) and the atlas-based procedure (Wang, et al, 2014). Most of them count on anatomical priors basically. Among the various segmentation methods, the atlas-based method needs the prior template of the human brain. The performance of morphology method might be related to the prior initial regional minima with the issue of over segmentation probably. Besides, using the image intensity information prior, the threshold selection in segmentation is sensitive to noise for images with low contrast in medical imaging (Tohka, 2014; Yang, et. al., 2015; Duyn, 2012). The review above reveals that most of the segmentation methods might be unsuccessful in automated real time applications, which generally work with no human involvement and demand no any anatomical priors for image segmentation. Different from the segmentation methods reviewed above, this study aims to use an image-based color region growth procedure for image pattern segmentation, as to address the issue of detecting positions of disease-related patterns with color visualization of shape graphically in medical imaging, including epilepsy in SEEG and brain tumors in MRI.

II. PROPOSED METHOD

Figure 1 illustrates the proposed image-based locator using the graphic color region growth procedure for segmentation (CRGPS), in order to detect positions of disease-related pattern with color visualization of shape graphically in medical imaging. In the CRGPS approach, the segmentation **S** is a partition of a color image into graphic regions of color such that each graphic region of color $\mathbf{R} \in \mathbf{S}$ corresponds to a connected graphic region in the color image. This means that the segmentation in the CRGPS approach is induced by a subset of the graphic regions of color in the color image.

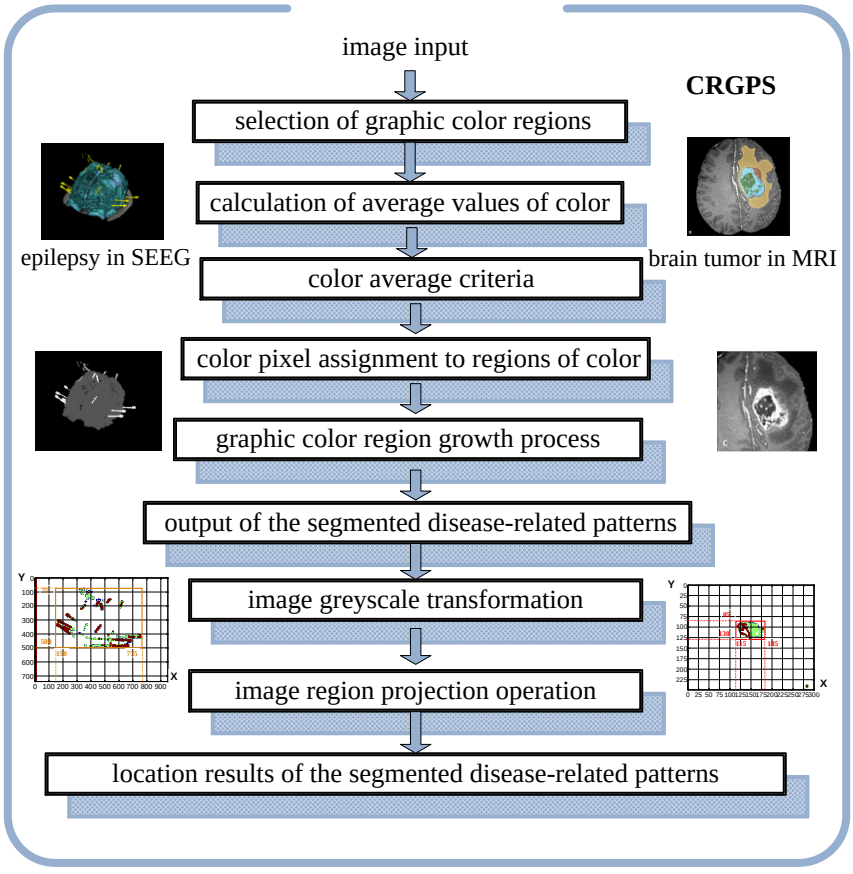

Figure 1: Proposed method

In image processing, the segmentation is the process of partitioning an image into various segments of image patterns, in order to change the representation of an image into objects of interest that is more meaningful and easy to analyze. For a color image, the segmentation is the procedure of assigning a pattern label to each color pixel such that color pixels with the same pattern label share certain characteristics with color. One

technique of the graphic color region growth procedure for segmentation counts on mainly on the hypothesis that the neighboring pixels within one color region have similar values. In general, the differences among intensity values of color pixels and the average values of colors in the color regions in a color image are used as criteria to measure the likeness among them. This means that the pixel with the smallest difference measured in this way is assigned to the respective color region in a color image. This process continues until all pixels are assigned to a color region (Rafael, et al., 2008; Petrou, et al., 2004).

Image segmentation can be applied further to locate objects of interest, i.e., some disease-related patterns in medical imaging. The graphic color region growth procedure is an effective technique for image segmentation, which models the impact of pixel neighborhoods on a given color region of pixels or pixel under the hypothesis of homogeneity in color images. In the proposed CRGPS approach, the graphic color region growth procedure is employed as a main process that partitions a color image into graphic regions of color, in order to detect positions of segmented disease-related patterns. Given a set of *n* regions of color in a color image, $\mathbf{R}$ **(**r_1**,** $r_{2, \ldots\ldots, }$ r_n), the graphic color region growth procedure is an approach to determining the *n* regions of color basically by the formulation (Rafael,et al., 2008; Petrou, et al., 2004; Moon, et al., 2000):

$$(\mathrm{A}) \qquad \mathbf{R} = \sum_{i=1}^{n} r_i \; ; \quad \text{and}$$

$$(\mathrm{B}) \qquad P(r_i) = \text{True} \qquad \text{for} \quad i = 1, 2, \ldots\ldots n.$$

The formula (A) indicates that the graphic color region growth procedure in a color image, $\mathbf{R}$ **(**r_1**,** $r_{2, \ldots\ldots, }$ r_n), must be complete thoroughly. In other words, each color pixel must be located in a graphic region of color, r_i (i = 1, 2, ……, n), in the procedure; in the formula (B), the properties of color in the procedure need to be satisfied by the color pixels within a segmented color region.

Because an image with color could have at least three color components, each color pixel in the color image could be considered as a vector of color components in a coordinate system. For example, each color pixel in the RGB (red, green and blue) coordinate system can be characterized as a vector of the RGB components, from the origin to that pixel in the RGB coordinate system**.** In this study, we let the average values of color be denoted by the RGB vectors as a set of seed points of pixels in the graphic color region growth procedure in the color image. Given a set of color pixels representative of a color (or the range of color) of interest in the color image, we could get an estimate of the average values of color, defined as the color average criteria in the graphic color region growth procedure. In this study, based on the predefined color average criteria, the graphic color region growth procedure checks adjacent color pixels of the neighboring points and evaluate whether the adjacent color pixel would be joined in graphic regions of color. If the predefined color average criteria is satisfied, the color pixel would be set to the color region as one or more of its neighbors.

By way of the color average criteria using the Euclidean distance, the graphic color region growth procedure needs to calculate each color pixel in the set of properties of color, $P(r_i)$, for assignment of that color pixel to a graphic sub-region of color, r_i. The shortest distance indicates that there is the positive underlying likeness of color between that color pixel and the one alike graphic sub-region of color in the graphic color region growth procedure. In summary, the main steps in the CRGPS approach are the following: (1) calculate average values of colors of patterns as the predefined color average criteria; and (2) allocate each color pixel to a region of color in the graphic color region growth procedure, according to the color average criteria, until there are no modification in two successive iterative steps in the procedure.

Greyscale images have shades of grey with the spectrum of grey monochrome regardless of its color in the context of computer imaging. Pattern pixels in greyscale image could be quantized to be stored as rational numbers for computation. To locate the positions of segmented color regions of patterns in the X-Y coordinate plane, the image greyscale transformation is performed first to characterize segmented patterns in the levels of grey with rational numbers in computation. Then, accomplished by the image region projection operation, the proposed CRGPS approach enables to locate positions of segmented disease-related patterns of interest in the X-Y coordinate plane, including multiple intracranial electrodes implanted for the detection of the SOZ for epilepsy in SEEG and brain tumors in MRI in the validation.

III. EXPERIMENTAL RESULTS

This section is divided into two subsections in the CRGPS implementation on the experimental datasets of the epilepsy image in SEEG and the brain tumor image in MRI. In the first subsection, a set of segmentation results is reported to assess the performance of the proposed CRGPS method for image pattern segmentation with graphic color visualization of shape. The second one presents the location results for detecting the graphic regions of the segmented multiple electrodes implanted for the detection of the SOZ with epilepsy and the segmented necrotic/cystic core pattern for brain tumors in the X-Y coordinate plane.

3.1 Image Segmentation Results

Figure 2 presents the segmentation results from an example of experiments in an epilepsy image in SEEG in the CRGPS implementation. Figure 2(a) is the original image of epilepsy in SEEG (Image credit: McGill University). The original image size is of 300 X 249 pixels of color. It can be observed that there are five different colors of image patterns graphically in the original color image (with the image patterns of the yellow, the grey, the blue, the green and the purple), indicating five graphic sub-regions of color needed to be selected in the graphic color region growth procedure.

Achieved by the CRGPS implementation in this study, Figure 2(b) shows the segmentation results with the output of the five visible segmented image patterns, 'A', 'B', 'C', 'D' and 'E' on the epilepsy image dataset in SEEG. In Figure 2(b), the segmented brain anatomy section 'B' is shown in grey color, while the other three segmented patterns of brain_markups ('C', 'D', and 'E') are separated graphically in the blue color, the green color and the purple color, respectively. More importantly, we can see that the segmented pattern of multiple intracranial electrodes 'A' in Figure 2(b) is shown clearly in yellow color with visualization of shape graphically, which was implanted for detecting the location of the SOS which might assist in diagnosing the type of an epilepsy.

Figure 3 shows the segmentation results from an example of experiments in the brain tumor image in MRI in the CRGPS implementation. Figure 3(a) is the original image of brain tumor in MRI (Image credit: University of Pennsylvania). The original image size is of 326 X 306 pixels. In Figure 3(a), there are five different colors of graphic image patterns, the green one (the necrotic/cystic core), the blue one (enhancing core), the yellow one (the edema), the red one (the non-enhancing solid core) and the grey one (brain anatomy section), involved in the original image of brain tumor in MRI; this means that five graphic sub-regions of color are needed to be selected in the graphic color region growth process for the image of brain tumor in MRI.

Figure 3(b) displays the segmentation results with the output of the five visible segmented patterns, 'A', 'B', 'C', 'D' and 'E', achieved in the CRGPS implementation on the brain tumor image in MRI. It can be seen that the results of the five segmented pattern sections are shown graphically in various of colors, the graphic patterns of green 'A', the blue 'C', the yellow 'D' and the red 'E', plus the brain anatomy pattern 'B' with grey color. Among them, the graphic pattern of green 'A' is the necrotic/cystic core in brain tumors whose position usually needs to be located precisely for the medical intervention.

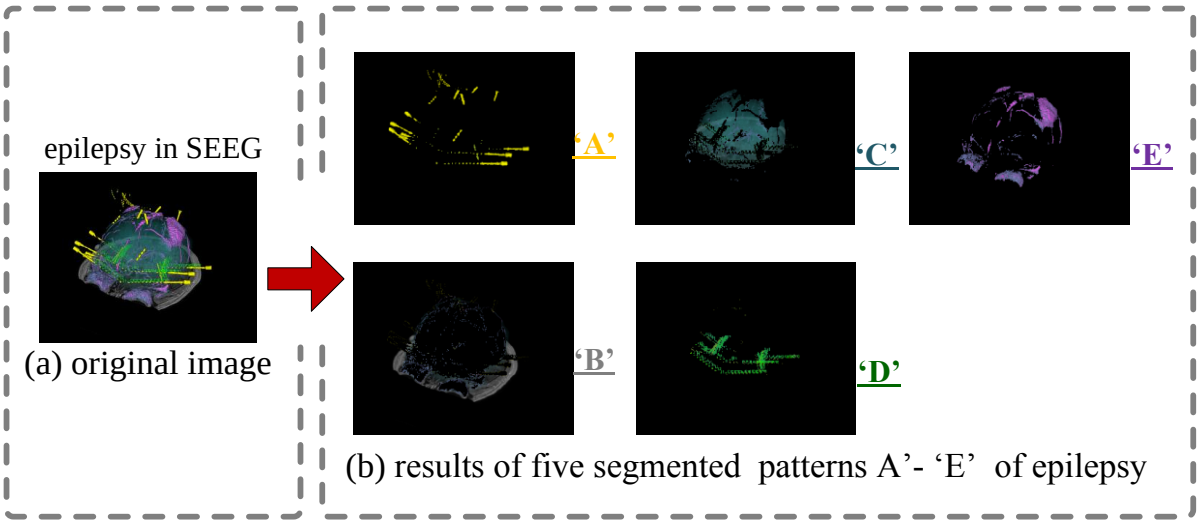

Figure 2: Segmentation results from an example of experiments in an epilepsy image in SEEG: (a) the original epilepsy image in SEEG (Image credit: McGill University); (b) segmentation results of the five segmented image patterns graphically.

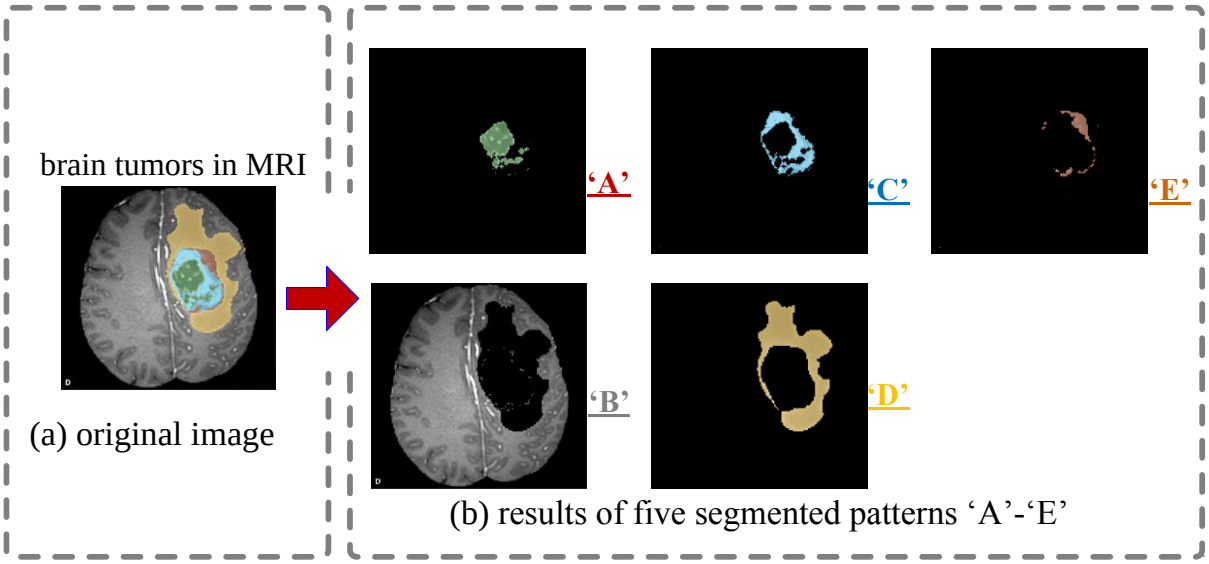

Figure 3: Segmentation results from an example of experiments in the brain tumor image in MRI: (a) original brain tumor image in MRI (Image credit: University of Pennsylvania); (b) segmentation results of the five segmented image patterns.

3.2 Location Results for the Segmented Image Pattern Positions

In the scenarios, the proposed CRGPS approach in this study is interactive, which integrates the technique in the graphic color region growth procedure for segmentation and the model for detecting locations of segmented disease-related patterns graphically in the X-Y coordinate plane. After the color image partitions into the meaningful pattern regions of color (see Figures 2-3(b)), Figures 4-5 further illustrate the location results in the CRGPS implementation for each of segmented patterns 'A' from Figures 2-3(b), the segmented implanted electrodes pattern 'A' with yellow for epilepsy in Figure 2(b) and the segmented necrotic/cystic core pattern 'A' with red for brain tumors in Figure 3(b).

Greyscale images are composed exclusively of shades of grey. In greyscale image, the intensity of a pixel is represented in a given range from 0% to 100% with any rational numbers in between. In greyscale images, each pixel depth allows 256 different intensities (indicating of shades of grey) to be recorded, which simplifies the computation in the applications of image processing. In this study, the image greyscale transformation is performed to convert the two segmented color patterns 'A' {from Figures 2-3(b)} to grayscale images in the levels of grey. Figures 4-5(a) show their image transformation results of the two segmented patterns 'A' in greyscale in a range of monochromatic shades from black to white with their rational numbers. Therefore, each sample pattern in greyscale images in Figures 4-5(a) can be accessed individually as one full byte in the computation through their rational numbers, which are used for locating the position of these two graphic segmented pattern 'A' in the X-Y coordinate plane.

Using the operation of image region projection, Figures 4-5(b) further illustrate the location results for detecting the positions of the two segmented pattern 'A' in the X-Y coordinate plane, where the segmented intracranial electrodes pattern 'A' for epilepsy located in the position {(x1, x2), (y1, y2) = (150, 775), (75, 500)} within the yellow rectangle in Figure 4(b) and the segmented necrotic/cystic core pattern 'A' for brain tumors located in the position {(x1, x2), (y1, y2) = (170, 245), (110, 185)} within the green rectangle in Figure 5(b). As a result, this would be helpful to have unique insight to probe the depths of regions of seizure focus in SEEG and brain tumors in MRI graphically for the early medical intervention.

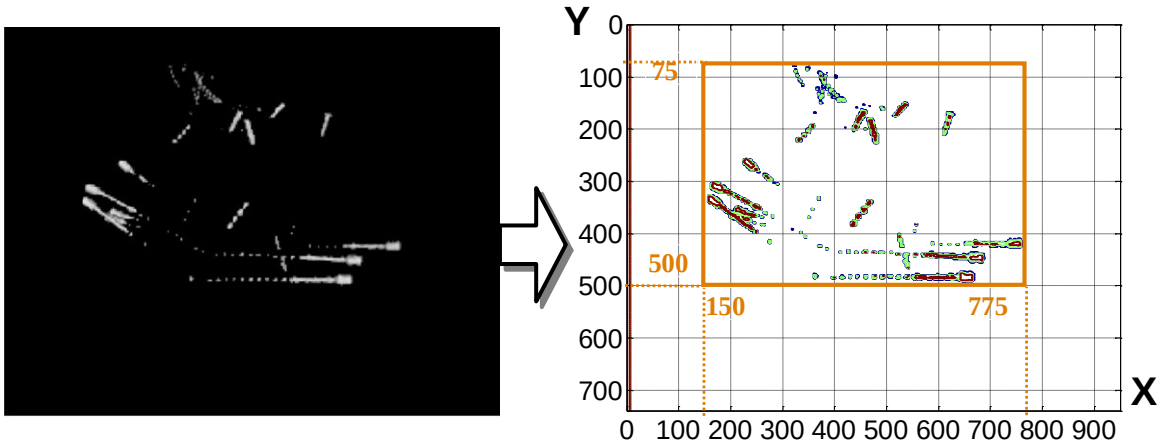

(a) results of the segmented electrodes pattern 'A' from Fig. 2(b) in greyscale;

(b) location results for segmented electrodes pattern 'A' in yellow rectangle {(150, 775), (75, 500)}.

Figure 4: Location results for the segmented implanted intracranial electrodes pattern 'A' (the one with yellow in Figure 2(b)) in the X-Y coordinate plane in the CRGPS implementation.

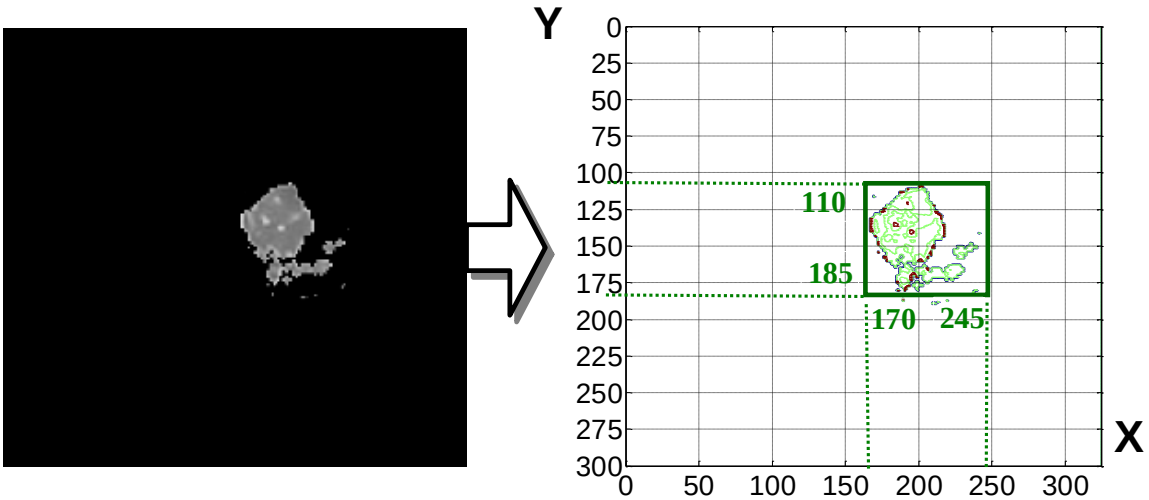

(a) results of the segmented necrotic/cystic core pattern 'A' of brain tumor from Fig. 3(b) in greyscale;

(b) location results for segmented necrotic/cystic core pattern 'A' of brain tumor in green rectangle {(170, 245), (110, 185)}.

Figure 5: Location results for the segmented brain tumor pattern 'A' (the one with green in Figure 3(b)) in the X-Y coordinate plane in the CRGPS implementation.

IV. DISCUSSION AND CONCLUSION

The SOZ for the brains of people with epilepsy is an electroclinical definition associated with the site of beginning and of the primary organization of the seizures in cerebral regions with the seizures. Symptoms vary depending on the type of seizure. One main hypothesis is that the SOZ is located in the right insula related to the large insular tuber with propagation in the anterior cingulate cortex. There is also the possibility of either early involvement of the frontal lobe or a purely frontal SOZ involving the anterior cingulate cortex. In general, it is not easy to locate precisely the insular extension of the SOZ, where the seizure propagates through pre-surgical evaluations (Wang, et al., 2021; Despouy, et al., 2019; Bartolomei et al., 2017).

Detecting the regions of the disease related-patterns of interest in medical imaging would be helpful for medical interventions in neurological diseases. In this study, the implementation results show that the proposed CRGPS locator is capable of detecting graphic regions of disease-related patterns for discovering valuable information for the implanted electrodes in localizing the SOZ. For example, in the original image of epilepsy in SEEG in Figure 2(a), the implanted electrodes pattern 'A' (with obscure yellow points of line) was hidden there under the brain mark-up pattern 'C' (with the blue region of area); however, without hidden by the brain mark-up pattern 'C' as achieved from the CRGPS implementation, the implanted electrodes pattern 'A' in Figure 2(b)

can be seen clearly in yellow color individually, ultimately leading to localization of the implanted electrodes pattern 'A' with visualization of shape graphically in the X-Y coordinate plane (see Figure 4) in this study.

This study is the first to explore an approach to locate intracranial electrodes implanted for the SOZ and brain tumors with an improved visualization of shape using the graphic color region growth procedure for segmentation in medical imaging. Although the current proposed CRGPS method has a limitation of the shortage of medical image data used in the implementation, this can be solved by implementing more neuro-images with access to bigger data sets of medical imaging. The experimental results show the clinical applicability of the proposed CRGPS method for locating positions of the segmented image patterns in the X-Y coordinate plane graphically in both of the brain tumor image in MRI and the epilepsy image in SEEG. This would allow to intervene with therapies in the step where can personalize in the way that might be meaningful in the diagnoses of disease.

Detecting the locations of disease related-patterns at combining approaches of image pattern segmentation might be helpful to diagnose neurological diseases in the early stage in medical imaging (Guo, 2017; Fereshtehnejad, et al., 2017; Lozano, et al., 2017; Martono, et al., 2016). In the future, more comparisons with other approaches in the literature on the data of epilepsy in SEEG and brain tumors in MRI might be possible in the access to more datasets of medical imaging. The research project in this study might have the potential to be applied for future models at combining new approaches to detect locations of disease-related patterns of interest graphically as markers for the early diagnoses of neurological diseases in medical imaging.

REFERENCES

[1]. Ahmed, W. and Fan, L. Analyze physical design process using big data tool: hidden patterns, performance measures, predictive analysis and classifying logs, *Int'l J. Software Science and Computational Intelligence*, 7(2), pp. 31-49, 2015.

[2]. Bauer, S., Wiest, R., Nolte, L.-P., Reyes, M. "A survey of MRI-based medical image analysis for brain tumor studies," *Phys. Med. Biol.*, vol. 58, pp. R97–R129, 2013.

[3]. Bakas, S, Akbari, H, Sotiras, A, Bilello, M, Rozycki, M, Kirby, J, Freymann, J, Farahani, K, Davatzikos, C. Segmentation Labels and Radiomic Features for the Pre-operative Scans of the TCGA-GBM collection. *The Cancer Imaging Archive*, 2017. (DOI:10.7937/K9/TCIA.2017.KLXWJJ1Q)

[4]. Bartolomei, F., Lagarde, S., Wendling, F., McGonigal, A., Jirsa, V, Guye, M., et al. Defining epileptogenic networks: Contribution of SEEG and signal analysis. *Epilepsia*, vol. 58, pp. 1131-1147, 2017.

[5]. Bahi-Buisson, N., Guttierrez-Delicado, E., Soufflet, C., Rio, M., Daire, VC., Lacombe, D., Héron, D., Verloes, A., Zuberi, S., Burglen, L., Afenjar, A., Moutard, ML., Edery, P., Novelli, A., Bernardini, L., Dulac, O., Nabbout, R., Plouin, P., Battaglia, A. Spectrum of epilepsy in terminal 1p36 deletion syndrome. *Epilepsia*, vol. 49, pp. 509-515, 2008.

[6]. Bi, H., Tang, H., Yang, G., Shu, H., and Dillenseger, J.-L. Accurate image segmentation using Gaussian mixture model with saliency map," *Pattern. Anal. Applic.*, vol. 21, pp. 869-878, 2018.

[7]. Chen, Y.-J., Liu, C.-M., Y.-C. Hsu, Y.-C. Lo, T.-J. Hwang, H.-G. Hwu, Y.-T. Lin, and W.-Y. I. Tseng. Individualized Prediction of Schizophrenia Based on the Whole-Brain Pattern of Altered White Matter Tract Integrity. *Hum. Brain Mapp.*, vol. 39, pp. 575-587, 2018.

[8]. Devi, C. N., Chandrasekharan, A., Sundararaman, V. K., Alex, Z. C. Neonatal brain MRI segmentation: A review. *Compu in Biology and Medicine*, vol. 64, no. 1, pp. 163–178, 2015.

[9]. Despouy, E., Curot, J., Denuelle, M., Deudon, M., Sol, J.-C., Lotterie, J.-A., Reddy, L., Nowak, L. G., Pariente, J., Thorpe, S. J., Valton, L., Barbeau, E. J. Neuronal spiking activity highlights a gradient of epileptogenicity in human tuberous sclerosis lesions. *Clin. Neurophysiol.*, vol. 130, pp. 537-47, 2019.

[10]. Duyn J. H. The future of ultra-high field MRI and fMRI for study of the human brain. *Neuroimage*, vol. 62, pp. 1241-1248, 2012.

[11]. Egger, J., Kapur, T., Fedorov, A., Pieper, S., Miller, JV., Veeraraghavan, H., Freisleben, B., Golby, AJ., Nimsky, C., Kikinis, R. GBM Volumetry using the 3D Slicer Medical Image Computing Platform. *Science Reports*, 1364, pp. 1-7, 2013.

[12]. Fereshtehnejad, SM, Zeighami, Y, Dagher, A, Postuma, RB. Clinical criteria for subtyping Parkinson's disease: biomarkers and longitudinal progression. *Brain*, pp. 1959-1976, 2017.

[13]. Guo, P., Evans, A. and Bhattacharya, P. Nuclei segmentation for quantification of brain tumors in digital pathology images," *Int'l J. Software Sci. and Comput. Intell.*, vol. 10, pp. 36-49, 2018.

[14]. Guo, P. A tissue-based biomarker model for predicting disease patterns," *J. Knowledge-Based Sys.*, vol. 276, pp. 160-169, 2017.

[15]. Gui, L., Lisowski, R. Faundez, T. Huppi, P. S. Lazeyras, F. and Kocher, M. Morphology-driven automatic segmentation of MR images of the neonatal brain, *Medical Image Analysis*, vol. 16, pp. 1565–1579, 2012.

[16]. Gerard, IJ., Kersten-Oertel, M., Petrecca, K., Sirhan, D., Hall, JA., and Collins, DL. Brain shift in Neuronavigation of brain tumours: A review. *Medical Image Analysis*, vol. 35, pp. 403-420, 2017.

[17]. Grecoa, M., Ferrarab, P., Farelloc, G., Strianod, P., Verrottie, A. Electroclinical features of epilepsy associated with 1p36 deletion syndrome: A review. J. *Epilepsy Research*. vol. 139, pp. 92-101, 2018.

[18]. Lozano, F., Ortiz, A., Munilla, J., Peinado, A. Automatic computation of regions of interest by robust principal component analysis. Application to automatic dementia diagnosis. *J. Knowledge-Based Systems*, vol. 123, pp. 229-237, 2017.

[19]. Martono, NP., Yamaguchi, T., Maeta, T., Fujino, H., Kubota, Y., Ohwada, H. and Giovanneti, T. Clustering finger motion data from virtual reality-based training to analyze patients with mild cognitive impairment, *Int'l J. Software Science and Computational Intelligence*, 8(4), pp. 29-41, 2016.

[20]. Moon, T.K. and Stirling, W.C. Mathematical Methods and Algorithms for Signal Processing. Prentice Hall. 2000.

[21]. Pellegrino, G., Hedrich, T. Rasheda Arman Chowdhury, Hall, J. A., Dubeau, F., Lina, J. M., Kobayashi, E. and Grova, C. Clinical yield of magnetoencephalography distributed source imaging in epilepsy: a comparison with equivalent current dipole method. *Human Brain Mapping*, vol. 39, pp. 218-231, 2018.

[22]. Petrou, M. and Bosdogianni, P. *Image Processing the Fundamentals*, Wiley, UK, 2004.

[23]. Pepe A, Zhao L, Koikkalainen J, Hietala J, Ruotsalainen U, Tohka J. Automatic statistical shape analysis of cerebral asymmetry in 3D T1-weighted magnetic resonance images at vertex-level: application to neuroleptic-naïve schizophrenia. *Magn Reson Imaging*, vol. 31, pp. 676-687, 2013.

[24]. Rafael, R. C. and Wood, R. E., 2008. Digital Image Processing, third ed. Prentice Hall, NJ.

[25]. Ryvlin, P, Cross, JH, Rheims, S. Epilepsy surgery in children and adults. *Lancet Neurol.*, vol. 13, pp.1114–1126, 2014.

[26]. Sohrabpour, A, Lu, Y, Worrell, G and He, B. Imaging brain source extent from EEG/MEG by means of an iteratively reweighted edge sparsity minimization (ires) strategy. *NeuroImage*, vol. 142, pp. 27–42, 2016.

[27]. Tohka J. Partial volume effect modeling for segmentation and tissue classification of brain magnetic resonance images: A review. *World J Radiol*. vol.11, pp. 855-864, 2014.
[28]. Wang, J., Jing, B., Liu, R., Li, D., Wang, W., Wang, J., Lei, J., Yue Xing, Y., Yan, J., Loh, H. H., Lu, G., Yang, X. Characterizing the seizure onset zone and epileptic network using EEG-fMRI in a rat seizure model. *NeuroImage*, vol. 237, pp. 1–11, 2021.
[29]. Wang, J., Vachet, C., Rumple, A., Gouttard, S., Ouziel, C., Perrot, E., Du, G., Huang, X., Gerig, G., Styner, M. Multi-atlas segmentation of subcortical brain structures via the AutoSeg software pipeline. *Front. Neuroinform*., 8, 2014. http://dx.doi.org/10.3389/fninf.2014.00007.
[30]. West J, Warntjes JB, Lundberg P. Novel whole brain segmentation and volume estimation using quantitative MRI. *Eur Radiol*. vol. 22, pp. 998-1007, 2012.
[31]. Weiner MW, Veitch DP, Aisen PS, Beckett LA, Cairns NJ, Green RC, Harvey D, Jack CR, Jagust W, Liu E, Morris JC, Petersen RC, Saykin AJ, Schmidt ME, Shaw L, Shen L, Siuciak JA, Soares H, Toga AW, Trojanowski JQ. The Alzheimer's Disease Neuroimaging Initiative: a review of papers published since its inception. *Alzheimers Dement*., vol. 9, e111-194, 2013.
[32]. Willcocks, C. G., Jackson, P. T. G., Nelson, C. J., Nasrulloh, A. V. and Obara, B. Interactive GPU active contours for segmenting inhomogeneous objects, J. Real Time Image Process, vol. 7, pp. 2305-2318, 2019.
[33]. Yang, X., Minh, H. L., Cheng, T., Sung, K., H., and Liu, W. Automatic segmentation of renal compartments in DCE-MRI images. *Proceeding on MICCAI*, Germany, pp. 3-11, 2015.

Peifang Guo. "An Image-based Locator for Detecting Regions of Disease-Related Patterns with Color Visualization of Shape in Medical Imaging." *International Journal of Engineering Research and Development*, vol. 17(03), 2021, pp 35-42.